View metadata, citation and similar papers at core.ac.uk
brought to you by CORE
provided by Engineering Journal (Faculty of Engineering, Chulalongkorn University, Bangkok)

ENGINEERING JOURNAL

Article

Synthesis of Tobermorite from the Ash after Treatment of Asbesto-Containing Disaster Waste, and Its Removal Ability of Cs(I) from Aqueous Solution

Takaaki Wajima

Department of Urban Environment Systems, Graduate School of Engineering, Chiba University, 1-33, Yayoi-cho, Inage-ku, Chiba 263-8522, Japan
E-mail: wajima@tu.chiba-u.ac.jp

Abstract. Tobermorite was synthesized successfully from the ash, which was produced and detoxified from asbesto-containing disaster waste in great east Japan earth quake, by alkali hydrothermal treatment. Tobermorite synthesis was examined as a function of reaction temperature and NaOH concentration. The formation of tobermorite was identified in the product treated with 1-4 M NaOH solution at 130 and 180 °C, while no product phases was identified at 80 °C. With increasing reaction temperature, intensity of tobermorite phase in the product and Cs^+ removal ability of the product increase. The product, which was treated with 4 M NaOH at 180 °C for 20 h, revealed the high selective uptake for Cs^+ in saline water. The Cs^+ uptake of the product was extrapolated using Langmuir and Freundlich isotherm models, experimental data are found to fit Langmuir than Freundlich, and the calculated uptake amount was 0.51 mmol/g. The kinetics for Cs^+ uptake was tested for pseudo-second order reactions, and the rate constants of uptake were calculated. With increasing temperature of aqueous solution, the kinetics of uptake is almost same and the uptake amount of Cs^+ decreases. The product is expected to be used for Cs^+ removal from wastewater.

Keywords: Tobermorite, asbesto-containing disaster waste, Cs(I) removal, great east Japan earthquake.

ENGINEERING JOURNAL Volume 20 Issue 4
Received 3 March 2016
Accepted 13 June 2016
Published 1 August 2016
Online at http://www.engj.org/
DOI:10.4186/ej.2016.20.4.79

DOI:10.4186/ej.2016.20.4.79

1. Introduction

Due to their excellent thermal insulation properties, asbestos materials have long been used in a wide variety of industrial processes. However, such materials have been considered a general health hazard since the 1960s [1-3], and as a result, their use has substantially decreased in recent years. Nevertheless, challenges remain in the disposal of asbestos-contaminated waste materials, presenting a serious industrial and social concern. Mechanical milling [4, 5], plasma [6], fusion [7] and various other treatments [8-10] have been used to transform asbestos-contaminated materials into nonhazardous wastes. Anastasiadou *et al.* converted chrysotile asbestos into non-fibrous, nonhazardous materials such as forsterite using hydrothermal treatments at 300 – 700 oC and 1.75 – 5.80 MPa [4]. Colangelo *et al.* studied high-energy milling of asbestos-containing wastes and recycling of the asbestos-free powders obtained. They found that the powders obtained through high-energy milling of asbestos-cement waste were asbestos-free and could be profitably recycled in building materials [5]. Inaba *et al.* employed thermal plasma as a heating source to reduce the volume of fly ash with asbestos fibers [6]. Kodera *et al.* converted the mixture of asbestos waste and plastics waste into nonhazardous fused material using gasification [7]. These treatments methods have advantages as economically viable and safe commercial applications.

However, when major disasters strike urban areas, rapid detoxification technologies are needed to manage the resulting debris, particularly in countries with strict regulations governing the disposal of asbestos and other toxic waste materials. In such situations (e.g., the Great East Japan Earthquake of 11 March 2011), many older buildings destroyed in disasters may contain significant amounts of asbestos-contaminated cement tiles. To rapidly and efficiently detoxify such contaminated materials and return the affected areas to sustainable use while simultaneously adhering to applicable laws and regulations regarding toxic waste disposal, technologies capable of covering large amounts of asbestos-contaminated debris into nontoxic waste materials are urgently needed [11, 12]. However, this debris is the mixture of asbestos waste, woody waste, plastics waste, metal waste and so on. It is difficult to separate the asbestos from the mixture, except the separation of metal waste by gravimetric and magnetic methods. In this situation, we succeeded to convert the mixture of asbestos, woody waste and plastics into nonhazardous ash using gasification process [7]. It is expected as rapid detoxification technologies in the area affected by disaster, but the nonhazardous ash is discharged as wastes to dispose in landfill sites.

On the other hands, the principal long-term problem caused by nuclear accident is the contamination of the environment with radioactive ^{137}Cs, because cesium is very volatile and can be carried long distances [13]. Decontamination of the environment, humans, and animals is possible with the use of cesium-selective materials either by dispersion, for example, in water or soil, or by ingestion by humans and animals [13]. Different methods such as ion exchange, precipitation, solidification, and stabilization can be applied for remediation or treatment of soil and groundwater contaminated by Cs [14]. Among them, ion exchange using different materials is the most studied [14]. Much attention has been focused toward the uptake of Cs^+ on zeolites [15-18], clay minerals [13, 14, 19-22], and other adsorbents [23-27].

Tobermorite [$Ca_5Si_6(OH)_2O_6 \cdot 4H_2O$] is the most important compound in various hydrous calcium silicates and can act as a cation exchanger, in particular shows high selectivity for Cs^+. Tobermorite may thereby have myriad applications in catalysis, nuclear and hazardous waste disposal, and waste-water treatment [28, 29]. Considerable effort has been made in the synthesis of tobermorite from waste as such. Tobermorite has been synthesized from some ashes, such as rice husk ash [30], oil shale ash [31, 32], paper sludge ash [33, 34], coal fly ash [35], incinerated municipal waste fly ash [36] and blast furnace slag [37]. The material has been used as a cation exchanger in the decontamination of radioactive species from low-level nuclear wastes and for heat insulating and fire-resistant building materials [38, 39].

From these backgrounds, in this study, we attempted to synthesize tobermorite from the ash after gasification treatment of asbesto-containing disaster waste, and its removal ability of Cs(I) from aqueous solution was estimated to apply for treatment of the environmental contamination with radioactive Cs caused by nuclear accident.

2. Experimental

2.1. Raw Materials

Raw ash used in this study was collected from the practical test plant for treatment of asbesto-containing disaster waste [7]. The chemical composition of the ash is listed in Table 1. The ash contains ignition loss

(LOI) (6.0 %), mainly originated from unburned carbon, according to the results of differential thermal analysis (DTA) / thermogravimetry (TG) (TG8120, Rigaku, Japan), and predominantly CaO (36.2 %), SiO_2 (33.1 %), Na_2O (12.8 %) and Al_2O_3 (7.4 %), determined by X-ray fluorescence (XRF) (Primini, Rigaku, Japan).

Table 1. Chemical composition of the ash after treatment of asbesto-containing disaster waste.

Oxide	Composition (wt%)
CaO	36.2
SiO_2	33.1
Al_2O_3	7.4
MgO	6.4
Fe_2O_3	1.5
Na_2O	12.8
K_2O	0.5
SO_3	0.7
Cl	0.4
MnO	0.6
CuO	0.2
ZnO	0.1
SrO	0.1
LOI	6.0

2.2. Synthesis

The ash (2.5 g) were added to 0 – 4 M NaOH solutions (10 mL) in 50 mL pressure vessels. These vessels were heated and maintained at 80, 130 and 180°C for 20 h in an electric furnace. After heating, the vessel was quenched with tap water and the solid product was filtered, washed with distilled water and dried in a drying oven at 60°C overnight. Phase identification of the raw material and products was carried out using an X-ray powder diffractometer (XRD; RIGAKU, Ultima IV), morphological information was obtained from the scanning electron microscope (SEM; TOPCOM, SM-200M).

The Cs adsorption capacity of the products obtained was measured as follows. Each synthesized product (0.1 g) was added to 20 mL of 1 mM CsCl solution in a 50 mL polypropylene centrifuge tube, and the tube was shaken using a reciprocal shaker for 2 hours. After shaking, the aqueous phase was separated from the solid by centrifugation, the supernatant pH measured using a pH meter (HORIBA, D-53) and the concentration of Cs^+ in the supernatant determined using an atomic absorption spectrophotometers (AAS; Perkinelmer, AAnalyst 200). The amount of adsorbed Cs^+ on the product, q_e, was calculated from the decrease in Cs^+ concentration in the medium by considering the adsorption volume and amount of product used:

$$q_e = \frac{[(C_0 - C_e) \bullet V]}{m} \quad (1)$$

Here, q_e (mmol/g) is the amount of Cs^+ adsorbed onto the product unit mass at equilibrium; C_0 and C_e are the Cs^+ concentrations in the initial solution and aqueous phase after treatment for a certain adsorption time, respectively (mM); m is the mass of product used and V is the Cs solution volume (L).

2.3. Adsorption studies

The effect of initial Cs^+ concentration on product adsorption capacity was determined using solutions of concentration ranging from 1 to 10 mM. Again, 0.1 g of product was added to 20 mL Cs^+ solution in the tube at room temperature and the tube was shaken for 3 h. After shaking, the aqueous phase was separated from the solid by centrifugation, the Cs^+ supernatant concentration determined by AAS, q_e was determined.

To determine the adsorption rate of Cs^+ from aqueous solution, 1 g of product was added to 200 mL of a 2.5 mM CsCl solution and stirred using a magnetic stirrer at 25, 35 and 45°C. While stirring, 2 mL aliquots were removed from the solution and the Cs^+ concentration in the filtrate determined by AAS to calculate q_e.

Selectivity of Cs^+ removal in salty solution was determined using diluted seawater. Seawater was diluted to 0 – 1000 times, and then CsCl powder was added to adjust 0.25 mM CsCl concentration. The product (0.1 g) was added to 20 mL of these solutions in a 50 mL polypropylene centrifuge tube, and the tube was shaken using a reciprocal shaker for 3 hours. After shaking, the aqueous phase was separated from the solid by centrifugation, the supernatant pH measured using a pH meter and the concentration of Cs^+ in the supernatant determined using an AAS. The Cs^+ removal using the product, *R*, was calculated as follows:

$$R = \frac{C_0 - C_e}{C_0} \times 100 \quad (2)$$

It is noted that pH of the solution after shaking is approximately 9.

3. Results and Discussion

3.1. Tobermorite Synthesis

The product phases synthesized from the ash under various experimental conditions are shown in Table 2. The tobermorite phase [$Ca_5Si_6(OH)_2O_{16}{\cdot}4H_2O$] can be synthesized from the ash above 130°C, while no product phases can be obtained at 80°C.

Table 2. The product phase on experimental various conditions.

Temperature (°C)	NaOH concentration (M)	Product phase
80	1	None
	2	None
	3	None
	4	None
130	1	Tobermorite
	2	Tobermorite
	3	Tobermorite
	4	Tobermorite
180	1	Tobermorite
	2	Tobermorite
	3	Tobermorite
	4	Tobermorite

XRD spectra of the raw ash and typical synthesis products, which was synthesized in 4 M NaOH at 180 °C, are shown in Figure 1. The main phases in the raw ash are crystalline quartz [SiO_2], larnite [$CaSiO_4$], calcite [$CaCO_3$], dolomite [(Ca, Mg) (CO_3)$_2$] and amorphous phases (Fig. 1(a)). The tobermorite phases appear as new peaks in the product, while those of quartz and other mineral phases in the ash diminished. It is believed that quartz and other mineral phases in the ash dissolve in the alkali solution to crystallize tobermorite phases under the hydrothermal conditions.

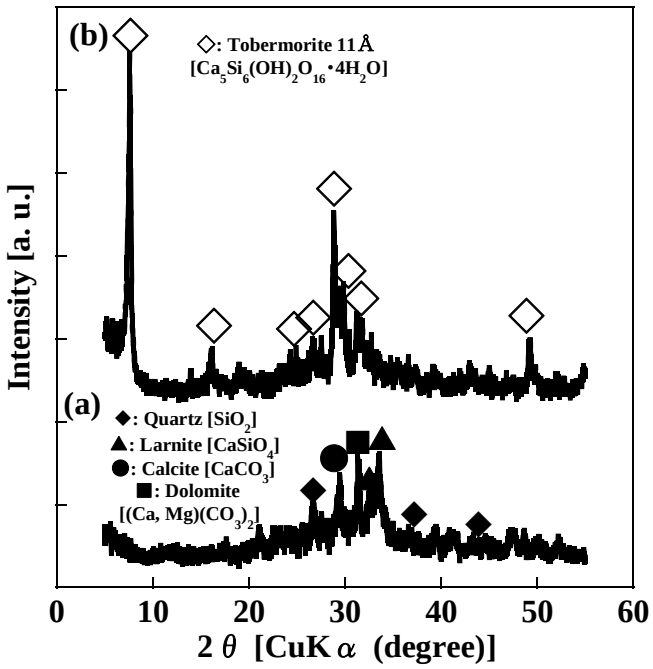

Fig. 1. XRD patterns of (a) raw ash and (b) the product synthesized in 4 M NaOH solution at 180 °C.

The SEM micrographs of the (a) the ash and (b) the product synthesized 4 M NaOH solution at 180 °C are shown in Figure 2. Although the raw ash consists of spherical or elliptical particles with smooth surface as shown in Figure 2 (a), the products are particles with platy crystals of tobermorite, as shown in Fig. 2 (b).

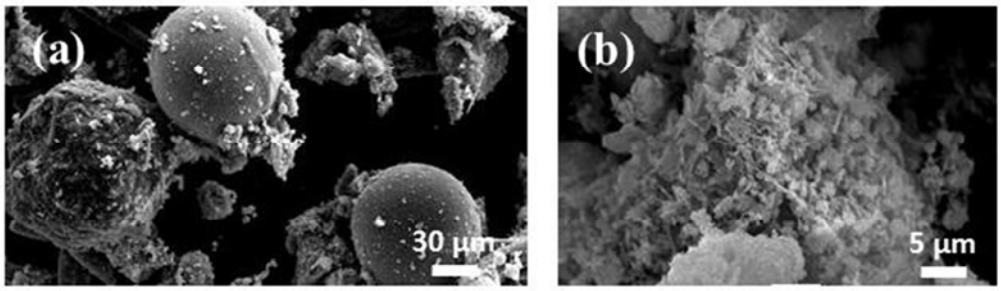

Fig. 2. SEM photos of (a) raw ash and (b) the product synthesized in 4 M NaOH solution at 180 °C.

The X-ray diffraction intensities of tobermorite in the product at given diffraction faces (0 0 2) are shown in Fig. 3. With increasing the reaction temperature, intensity of tobermorite in the product increases. In this experiment, the product with the highest intensity of tobermorite is obtained in 4 M NaOH solution at 180 °C.

DOI:10.4186/ej.2016.20.4.79

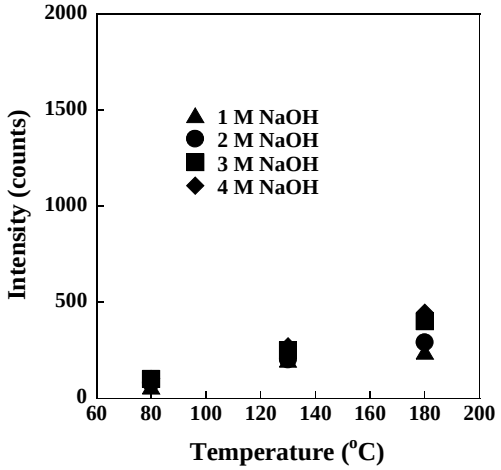

Fig. 3. Intensity of tobermorite in the products synthesized on various conditions.

The Cs adsorption ability of products synthesized from the ash under various experimental conditions is shown in Figure 4. Cs adsorption ability increased with increasing reaction temperature, while that is almost constant regardless of NaOH concentration. The product with high Cs adsorption ability was obtained at 180°C, due to the presence of tobermorite phases in the product.

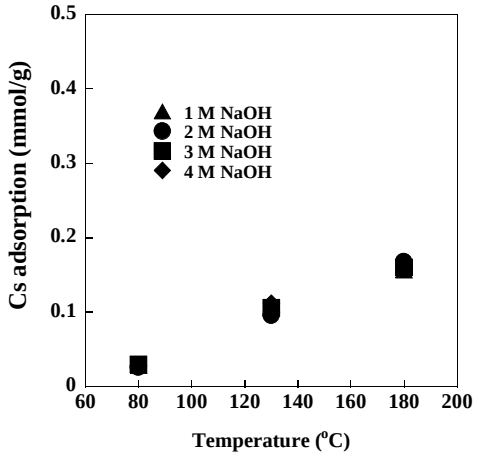

Fig. 4. The Cs adsorption ability of the product synthesized on various conditions.

3.2. Cs(I) Adsorption

The properties of Cs^+ adsorption for the product synthesized in 4 M NaOH solution at 180 °C were examined. The isotherm for Cs^+ adsorption using the product is shown in Figure 5. With increasing the equilibrium concentration, the adsorption for Cs^+ in the product steeply increases, and then gradually increases. These results indicate that energetically less favorable sites become involved with increasing Cs^+ concentration in the aqueous solution.

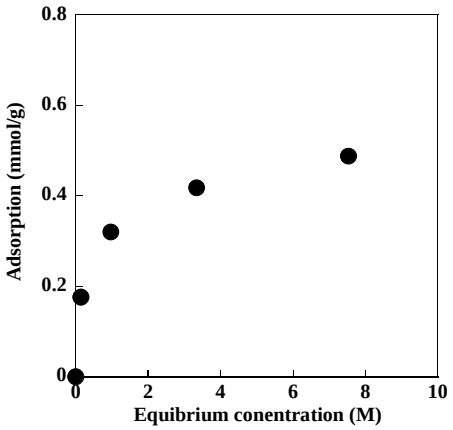

Fig. 5. Isotherm of Cs^+ using the product.

The equilibrium distribution of Cs^+ between the adsorbent and the solution is important in determining the maximum sorption capacity. Several isotherm models are available to describe the equilibrium sorption distribution where two models are used to fit the experimental data: the Langmuir and Freundlich models.

The linear form of the Langmuir model is given by:

$$\frac{C_e}{q_e} = \frac{1}{(q_{\max} \bullet K_L)} + \frac{1}{q_{\max}} C_e \tag{3}$$

where q_{max} (mmol/g) and K_L (L/mmol) are Langmuir constants related to the maximum adsorption capacity corresponding to complete coverage of the available adsorption sites and a measure of adsorption energy (equilibrium adsorption constant), respectively. These constants are found from the slope and intercept of the linear plot of C_e/q_e vs. C_e so that q_{max} = 1/slope and K_L = slope/intercept.

The linear form of the Freundlich model is also given by:

$$\ln(q_e) = \ln(K_F) + \frac{1}{n} \ln(C_e) \tag{4}$$

where K_F and n are Freundlich constants determined from the slope and intercept of the plot of $\ln(q_e)$ vs. $\ln(C_e)$.

The Langmuir and Freundlich isotherm models were applied to the experimental data as presented in Figure 5 and parameters calculated by each isotherm model are shown in Table 3. Our experimental results provide a correlation regression coefficient (R^2) as a measure of the goodness-of-fit. The Langmuir model fits the data better than the Freundlich model as the former has a higher correlation regression coefficient. q_{max}, as calculated from the Langmuir isotherm model, is 0.51 mmol/g. The cation exchange capacities (CECs) for the product are located at the lower end of the CEC range (0.59-1.97 mmol/g) reported for bespoke Al-substituted 11 Å tobermorites [28, 29, 38, 41]. Furthermore, tobermorite synthesized from coal fly ash is 0.53 mmol/g adsorbent [42]. Therefore, a maximum adsorption capacity of 0.51 mmol/g is comparable to that obtained from coal fly ash.

Table 3. Parameters and correlation regression using Langmuir and Freundlich models.

	Value
Langmuir	
q_{max}	0.51
K_L	1.98
R^2	0.996
Freundlich	
n	3.82
K_F	0.30
R^2	0.986

DOI:10.4186/ej.2016.20.4.79

Figure 6 illustrates the adsorption of Cs^+ by the product during the reaction at 25, 35 and 45°C. The slopes of the lines joining the data points in the figure reflect the adsorption rates. For all temperatures, the amount of adsorbed Cs^+ increases rapidly and reaches an equilibrium value after 15 min. With decreasing solution temperature, the amount of Cs^+ adsorption is higher. Short adsorption times are favored for minimum energy consumption and the product is therefore efficient for Cs^+ removal when its very satisfactory short adsorption time is considered.

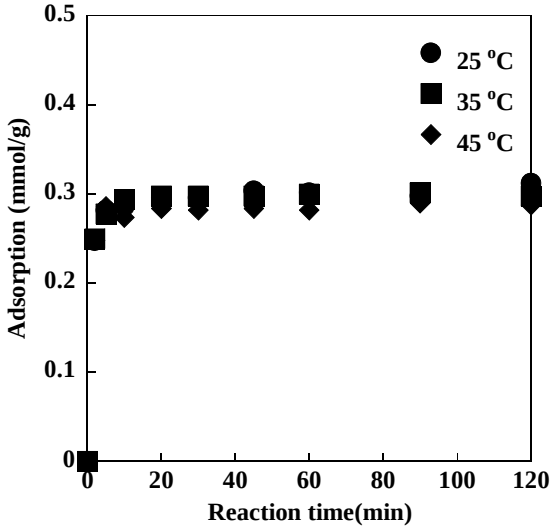

Fig. 6. The kinetics of Cs^+ adsorption using the product at 25, 35 and 45 °C.

The kinetic results obtained from batch experiments were analyzed using different kinetics models such as the Lagergren pseudo-first-order [43, 44] and pseudo-second-order models [45- 57]. The Lagergren pseudo-first-order model is given by:

$$\ln(q_e - q_t) = \ln(q_e) - k_1 \bullet t \tag{5}$$

where q_t is the amount of Cs^+ adsorbed on the product at any time (mmol of Cs^+/g product) and k_1 is the adsorption rate constant (min^{-1}). A linear plot of $\ln(q_e - q_t)$ against t gives the slope = k_1 and intercept = $\ln(q_e)$.

The equation that describes the pseudo-second-order model is given by the following linear form:

$$\frac{t}{q_t} = \frac{1}{(k_2 \bullet q_e^{\,2})} + \frac{1}{q_e} \bullet t \tag{6}$$

where k_2 is the adsorption rate constant (g/mmol min). k_2 and q_e are found from the intercept and slope of the plot of t/q_t vs. t so that q_e = 1/slope and k_2 = slope^2/intercept. The rate constants of the pseudo-first-order, k_1, and pseudo-second-order reactions, k_2, for Cs^+ adsorption were determined from Figure 6 and the values of k_1, k_2, R^2 (i.e. the linear correlation coefficient) and q_e (i.e. $q_{e,1}$ and $q_{e,2}$) are set out in Table 4. From the R^2 values it follows that the experimental data fit the pseudo-second-order model better than the pseudo-first-order model, which indicates that the adsorption process is second-order.

Table 4. Kinetics parameters and correlation regression using pseudo-first- and pseudo-second-order kinetics models.

	25 °C	**35 °C**	**45 °C**
Pseudo-first-order kinetics model			
$q_{e,1}$	0.053	0.054	0.050
k_1	0.071	0.175	0.108
R^2	0.838	0.948	0.997
Pseudo-second-order kinetics model			
$q_{e,2}$	0.31	0.30	0.29
k_2	3.5	14.4	6.8
R^2	0.999	1	1

It is evident that $q_{e,2}$ and k_2 are dependent on temperature. To gain insight into the thermodynamic nature of the adsorption process, several thermodynamic parameters were calculated. The Gibbs free energy change, $\Delta G°$, is negative, and the free energy of the adsorption reaction is given by the following equation:

$$\Delta G^0 = -RT \ln K_c \tag{7}$$

where K_c is the adsorption equilibrium constant, R is the gas constant (8.314 J/(mol · K)) and T is the absolute temperature (K). K_c can be calculated from:

$$K_c = \frac{F_e}{1 - F_e} \tag{8}$$

where F_e is the fraction of Cs^+ adsorbed at equilibrium and is obtained by the expression:

$$F_e = \frac{C_0 - C_e}{C_0} \tag{9}$$

where C_0 and C_e are the initial and equilibrium concentrations of Cs^+ in solution (mmol/L).

K_c for the adsorption of Cs^+ on the product was calculated at different temperatures and at equilibrium using Equations (8) and (9). The variation of K_c with temperature, as summarized in Table 5, showed that K_c decreased with increase in adsorption temperature, implying a strengthening of adsorbate-adsorbent interactions at lower temperature. Also, the obtained negative values of $\Delta G°$ confirm the feasibility of the process and the spontaneous nature of the adsorption process.

The Gibbs free energy can be represented as follows:

$$\Delta G^0 = \Delta H^0 - T \bullet \Delta S^0 \tag{10}$$

The enthalpy ($\Delta H°$) and entropy ($\Delta S°$) change calculated from the intercept and slope of the plot of $\Delta G°$ versus T are also given in Table 5. The change in $\Delta H°$ was found to be negative, confirming the exothermic nature of the adsorption process. The negative values of entropy ($\Delta S°$) show the decreased randomness at the solid/solution interface with some structural changes in the adsorbate and adsorbent.

DOI:10.4186/ej.2016.20.4.79

Table 5. Thermodynamic parameters and correlation regression for the adsorption of Cs^+ on the product.

Reaction temperature (K)	K_c	ΔG^0(kJ/mol)	ΔH^0(kJ/mol)	ΔS^0 (J/(mol·K)
298	1.48	-0.96		
308	1.36	-0.79	-6.58	-18.7
318	1.25	-0.59		

The selective removal of Cs^+ in saline water using the product was shown in Fig. 7. In distilled water with Cs^+ ion, the removal of Cs^+ indicates approximately 90 %, and in the solution diluted 1/100 and 1/1000 seawater, those are almost same value, while those in seawater and the solution diluted 1/10 seawater are 20 % and 65 %, which were lower than those in distilled water. Therefore, the product can selectively remove Cs^+ from river water and brackish water.

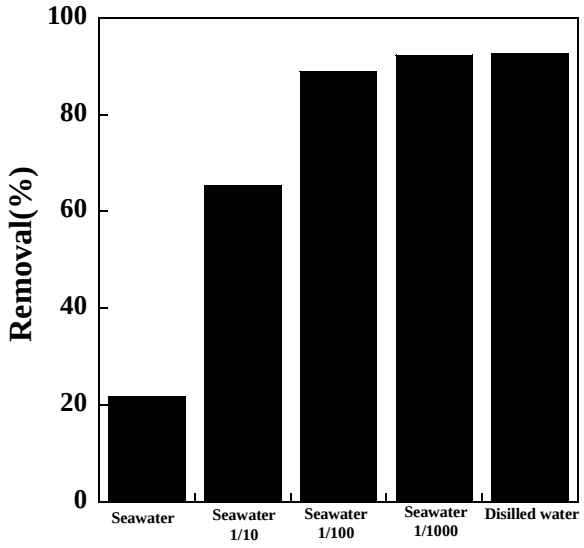

Fig. 7. The selective removal of Cs^+ in saline waste using the product.

4. Conclusion

We attempted to synthesize a tobermorite material from the ash after treatment of asbesto-containing disaster waste by hydrothermal treatment, and determined the Cs^+ adsorption ability of the product. Tobermorite can be synthesized from the ash using hydrothermal treatment, and the product containing tobermorite displayed the highest Cs^+ adsorption ability. The product has high selectivity for Cs^+ removal from saline water. The Langmuir and Freundlich adsorption isotherms were applied to equilibrium data, and the data were found to fit the Langmuir model. The maximum adsorption capacity of the product, as calculated from the Langmuir model, is 0.51 mmol/g. The Cs^+ adsorption kinetics from aqueous solution follows the pseudo-second-order model. The solution temperature influences Cs^+ adsorption; adsorption increased with a decrease in solution temperature. Cs^+ adsorption using the product is an exothermic and spontaneous process.

Acknowledgements

This work was partially supported by Industrial Technology Research Grant Program in P11014 from New Energy and Industrial Technology Development Organization (NEDO) of Japan, and Adaptable and Seamless Technology Transfer Program through Target-driven R&D, JST: 241FT0366.

References

[1] J. C. Wagner, C. A. Sleggs, and P. Marchand, "Diffuse pleural mesothelioma and asbestos exposure in the North Western Cape Province," *Br. J. Ind. Med.,* vol. 17, pp. 260-271, Oct., 1960.

[2] M. L. Newhouse, and H. Thompson, "Mesothelioma of pleura and peritoneium following exposure to asbestos in the London area, *Br. J. Ind. Med.,* vol. 22, pp. 261-269, Oct., 1965.

[3] I. J. Selikoff, and E. C. Hammond, "Environmental epidemiology. 3. Community effects of nonoccupational environmental asbestos exposure," *Am. J. Public Health,* vol. 58, no. 9, pp. 1658-1666, Sep., 1968.

[4] K. Anastasiadou, D. Axiotis, and E. Gidarakos, "Hydrothermal conversion of chysotile asbestos using near supercritical conditions," *J. Hazard. Mater.,* vol. 179, pp. 926-932, Jul., 2010.

[5] F. Colangelo, R. Cioffi, M. Lavorgna, L. Verdolotti, and L. D. Stefano, "Treatment and recycling of asbestos- cement containing waste," *J. Hazard. Mater.,* vol. 195, pp. 391-397, Nov., 2011.

[6] T. Inaba, M. Nagano, and M. Endo, "Investigation of plasma treatment for hazardous waste such as fly ash and asbestos," *Electr. Eng. Jpn.,* vol. 126, no. 3, pp. 73-81, Feb., 1999.

[7] Y. Kodera, K. Sakamoto, and H. Sekiguchi, "Development of detoxification fusion process for asbestos using fuel gas from waste plastics," E-Contechture, pp. 66-70, Sep., 2010 (In Japanese).

[8] Y. M. Chan, P. Agamuthu, and R. Mahalingam, "Solidification and stabilization of asbestos waste from an automobile brake manufacturing facility using cement," *J. Hazard. Mater.*, vol. 77, pp. 209-226, Oct., 2000.

[9] K. J. D. Mackenzie, and R. H. Meinhold, "A glass-bonded ceramic material from chrysotile," *J. Mater. Sci.*, vol. 29, pp. 2775-2783, May, 1994.

[10] A. F. Gualtieria, and A. Tartaglia, "Thermal decomposition of asbestos and recycling in traditional ceramics," *J. Eur. Ceram. Soc.*, vol. 20, pp. 1409-1418, Aug, 2000.

[11] Japan Ministry of the Environment (MOE), Guidelines (Master Plan) for DisasterWaste Management after the Great East Japan Earthquake, Japan MOE, Tokyo, 2011 (In Japanese).

[12] E. K. Lauritzen, "Emergency construction waste management," *Safety Sci.*, vol. 30, pp. 45-53, Oct.-Dec., 1998.

[13] S. Komarneni, and R. Roy, "A cesium-selective ion sieve made by topotactic leaching of phlogopite mica," *Science*, vol. 239, pp. 1286-1288, Mar., 1988.

[14] Y. Cho, and S. Komarneri, "Cation exchange equilibria of cesium and strontium with K-depleted biotite and muscovite," *Appl. Clay Sci.*, vol. 44, pp. 15-20, Apr., 2009.

[15] H. Mumura, and K. Akiba, "Adsorption behavior of cesium and strontium on synthetic zeolite P," *J. Nucl. Sci. Technol.*, vol. 30, pp. 436-443, Mar., 1993.

[16] H. Mimura, K. Yokota, K. Akiba, and Y. Onodera, "Alkali hydrothermal synthesis of zeolites from coal fly ash and their uptake properties of cesium ion," *J. Nucl. Sci. Technol.*, vol. 38, pp. 766-772, Feb., 2001.

[17] H. Mimura, M. Sato, K. Akiba, and Y. Onodera, "Selective uptake of cesium by ammonium molybdophosphate (AMP)-calcium alginate composites," *J. Nucl. Sci. Technol.*, vol. 38, pp. 872-78, Feb., 2001.

[18] K. Murakami, T. Wajima, T. Kato, K. Sugawara, and T. Sugawara, "Thermodynamic and kinetic studies on Cs^{+}- and Sr^{2+}-exchange in natural zeolite from Akita, Japan," *Toxicol. Environ. Chem.*, vol. 91, pp. 1023-1034, Aug., 2009.

[19] N. Suzuki, D. Yamamoto, N. Agaguchi, H. Tsuchiya, K. Aoki, and Y. Kanzaki, "The ion-exchange property of some layered inorganic materials with potassium ion, rubidium ion and cesium ion, and selective cesium ion-exchange of synthetic mica," *Bull. Chem. Soc. Jpn.*, vol. 73, pp. 2599-2603, Nov., 2000.

[20] N. Suzuki, T. Komuro, and Y. Kanzaki, "Interfering effect for the cesium ion-exchange property of sodium difluorotetrasilicate and sodium taeniolite by alkaline-earth metal ions," *Bull. Chem. Soc. Jpn.*, vol. 81, pp. 912-916, Jul., 2008.

[21] T. Kodama, T. Higuchi, T. Shimizu, K. Shimizu, S. Komarneni, W. Hoffbauer, and H. Schneider, "Synthesis of Na-2-mica from metakaolin and its cation exchange properties," *J. Mater. Chem.*, vol. 11, p. 2072-2077, Jul., 2001.

[22] K. Iijima, T. Tomura, and Y. Shoji, "Reversibility and modeling of adsorption behavior of cesium ions on colloidal montmorillonite particles," *Appl. Clay Sci.*, vol. 49, pp. 262-268, Jul., 2010.

[23] T. Sangvanich, V. Sukwarotwat, R. J. Wiacek, R. M. Grudzien, G. E. Fryxell, R. S. Addleman, C. Timchalk, and W. Yantasee, "Selective capture of cesium and thallium from natural waters and simulated wastes with copper ferrocyanide functionalized mesoporous silica," *J. Hazard. Mater.*, vol. 182, pp. 225-231, Oct., 2010.
[24] H. Mimura, and Y. Onodera, "Selective uptake and recovery of cesium ions by composite columns of ammonium molybdophosphate (AMP)-calcium alginate," *J. Nucl. Sci. Technol.*, vol. 39, pp. 282-285, Feb., 2002.
[25] C. C. Pavel, M. Walter, P. Poml, D. Bouexiere, and K. Popa, "Contrasting immobilization behavior of Cs+ and Sr2+ cations in a titanosilicate matrix" *J. Mater. Chem.*, vol. 21, pp. 3831-3837, Jan., 2011.
[26] M. J. Manos, and M. G. Kanatzidis, "Highly efficient and rapid Cs^+ uptake by the layered metal sulfide $K_{2x}Mn_xSn_{3-x}S_6$ (KMS-1)," *J. Am. Chem. Soc.*, vol. 131, pp. 6599-6607, Apr., 2009.
[27] R. Chitrakar, Y. Makita, and A. Sonoda, "Cesium ion exchange on synthetic birnessite ($Na_{0.35}MnO_2{\cdot}0.6H_2O$)," *Chem. Lett.*, vol. 40, pp. 1118-1120, Oct., 2011.
[28] S. Komarneri, and D. Roy, "Tobermorites: a new family of cation exchangers," *Science*, vol. 221, pp. 647-648, Aug., 1983.
[29] M. Miyake, S. Komarneri, and D. Roy, "Kinetics, equilibria and thermodynamics of ion exchange in substituted tobermorites," *Mater. Res. Bull.*, vol. 24, pp. 311-320, Mar., 1989.
[30] K. Inoue, S. Tsunematsu, and H. Yamada, "Removal characteristics of heavy metal ions by Al-substituted tobermorites," *Gypsum Lime*, vol. 229, pp. 413-418, Mar., 1990.
[31] J. Reinik, I. Heinmaa, J. P. Mikkola, and U. Kirso, "Hydrothermal alkaline treatment of oil shale ash for synthesis of tobermorites," *Fuel*, vol. 86, pp. 669-676, Mar.-Apr., 2007.
[32] J. Reinik, I. Heinmaa, J. P. Mikkola, and U. Kirso, "Synthesis and characterization of calcium-alumino-silicate hydrates from oil shale ash-Towards industrial applications-," *Fuel*, vol. 87, pp. 1998-2003, Aug., 2008.
[33] N. J. Coleman, and D. S. Brassington, "Synthesis of Al-substituted 11 Å tobermorite from newsprint recycling residue: feasibility study," *Mater. Res. Bull.*, vol. 38, pp. 485-497, Feb., 2003.
[34] N. J. Coleman, "Synthesis, structure and ion exchange properties of 11 Å tobermorite from newsprint recycling residue," *Mater. Res. Bull.*, vol. 40, pp. 2000-2013, Nov., 2005.
[35] W. Ma, and P. W. Brown, "Hydrothermal synthesis of tobermorite from fly ashes," *Adv. Cement Res.*, vol. 9, no. 33, pp. 9-16, Jan., 1997.
[36] Z. Yao, C. Tamura, M. Matsuda, and M. Miyake, "Resource recovery of waste incineration fly ash: Synthesis of tobermorite as ion exchanger," *J. Mater. Res.*, vol. 14, no. 11, pp. 4437-4442, Nov., 1999.
[37] Z. Jing, F. Jin, T. Hashida, N. Yamasaki, and H. Ishida, "Hydrothermal solidification of blast furnace slag by formation of tobermorite," *J. Mater. Sci.*, vol. 42, pp. 8236-8241, Oct., 2007.
[38] S. Komarneni, and D. M. Roy, "New tobermorite cation exchangers," *J. Mater. Sci.*, vol. 20, pp. 2930-2936, Aug., 1985.
[39] X. Huang, D. Jiang, and S. Tan, Novel hydrothermal synthesis method for tobermorite fibers and investigation on their thermal stability," *Mater. Res. Bull.*, vol. 37, pp. 1885-1892, Sep., 2002.
[40] S. Komarneni, D. M. Roy, and R. Roy, "Al-substituted tobermorite: shows cation exchange," *Cem. Concr. Res.*, vol. 12, pp. 773-780, Nov., 1982.
[41] Z. D. Yao, C. Tamura, M. Matsuda, and M. Miyake, "Resource recovery of waste incineration fly ash: Synthesis of tobermorite as ion exchanger" *J. Mater. Res.* vol. 14, pp. 4437-4442, Nov., 1999.
[42] Y. S. Ho, and G. McKay, "Comparative sorption kinetic studies of dye and aromatic compounds onto fly ash,". *J. Environ. Sci. Health, Part A: Toxic/Hazard. Subst. Environ. Eng.* vol. 34, pp. 1179-1204, Dec., 1999.
[43] Z. Aksu, "Equilibrium and kinetic modeling of cadmium (II) biosorption by C. vulgaris in batch system: effect of temperature," *Sep. Purif. Technol.* vol. 21, no. 3, pp. 285–294, Jan., 2001.
[44] Y. S. Ho, D. A. J. Wase, and C. F. Forster, "Kinetic studies of competitive heavy metal adsorption by sphagnum moss peat," *Environ. Technol.* vol. 17, no. 1, pp. 71–77, May, 1996.
[45] Y. S. Ho, and G. McKay, "A comparison of chemisorption kinetic models applied to pollutant removal on various sorbents," *Process Saf. Environ. Prot.* vol. 76, pp. 332–340, Nov., 1998.
[46] Y. S. Ho, and G. McKay, "Sorption of dye from aqueous solution by peat," *Chem. Eng. J.* vol. 70, no. 2, pp. 115–124 , Jun., 1998.
[47] Y. S. Ho, and G. McKay, "Pseudo-second order model for sorption processes, " *Process. Biochem.* vol. 34, no. 5, pp. 451–465 , Jul., 1999.

[48] Y. S. Ho, and G. McKay, "The kinetics of sorption of divalent metal ions onto sphagnum moss peat," *Water Res.* vol. 34, no. 3, pp. 735–742, Feb., 2000.
[49] M. Y. Arica, Y. Kacar, and O. Genc, "Entrapment of white rot fungus Trametes vesicolor in Ca-Al genate beads: preparation and biosorption kinetic analysis for cadmium removal from an aqueous solution," *Bioresour. Technol.* vol. 80, pp. 121–129, Nov., 2001.
[50] F. C. Wu, R. L. Tseng, and R. S. Juang, "Kinetic modeling of liquid-phase adsorption of reactive dyes and metal ions on chitosan," *Water Res.* vol. 35, no. 3, pp. 613–618, Feb., 2001.
[51] S. Azizian, "Kinetic models of sorption: a theoretical analysis," *J. Colloid Interface Sci.* vol. 276, no. 1, pp. 47–52, Aug., 2004.
[52] Y. S. Ho, "Comment on kinetic modeling and equilibrium studies during cadmium biosorption by dead Sargassum sp. Biomass by C.C.V. Cruz, A.C.A da Costa, C.A. Henriques and A.S. Luna," *Bioresour. Technol.* vol. 93, no. 3, pp. 321–324, Jul., 2004.
[53] Y. S. Ho, "Comments on arsenic removal using mesoporous alumina prepared via a templating method," *Environ. Sci. Technol.* vol. 38, no. 11, pp. 3214–3215, Apr., 2004.
[54] Y. S. Ho, "Comments on removal of copper from aqueous solution by aminated and protonated mesoporous aluminas: kinetics and equilibrium by S. Rengaraj, Y. Kim, C.K. Joo and J. Yi.," *J. Colloid Interface Sci.* vol. 276, no. 1, pp. 255–258, Aug., 2004.
[55] Y. S. Ho, "Comments on cadmium removal from aqueous solutions by chitin: kinetic and equilibrium studies," *Water Res.* vol. 38, no. 12, pp. 2962–2964, Jul., 2004.
[56] Y. S. Ho, "Comments on collagen-fiber-immobilized tannins and their adsorption of Au(III), " *Ind. Eng. Chem. Res.* vol. 43, no. 19, pp. 6265, Aug., 2004.
[57] K. C. Justi, M. C. M. Laranjeira, A. Neves, A. S. Mangrich, and V. T. Fa'vere, "Chitosan functionalized with 2[-bis-(pyridylmethyl)aminomethyl]4-methyl-6-formyl-phenol: equilibrium and kinetics of copper(II) adsorption," *Polymer,* vol. 45, no. 18, pp. 6285–6290, Aug., 2004.